Aerosol and Air Quality Research, 16: 1533–1540, 2016

ISSN: 1680-8584 print / 2071-1409 online
doi: 10.4209/aaqr.2015.08.0527

Theoretical Model for Normal Impact between Dry Sphere and Liquid Layer with Considerable Thickness

Jiliang Ma, Daoyin Liu*, Xiaoping Chen

Key Laboratory of Energy Thermal Conversion and Control of Ministry of Education, School of Energy and Environment, Southeast University, Nanjing 210096, China

ABSTRACT

Detailed understanding on the impact mechanism with presence of liquid is helpful for elucidating complex behaviors of wet particle flows. This paper has extended elastohydrodynamic theory by coupling the physical force models for the wet normal impact with a liquid layer of considerable thickness. The contact is divided into penetration, contact, and rebound stages. Three critical Stokes numbers are developed for each stage to predict the sphere rebound behavior. The dependence of the critical Stokes numbers on the layer thickness, sphere radius and the liquid viscosity is also studied. When the layer thickness and liquid viscosity ranges within a low level, most of the kinetic energy is dissipated in the contact stage. With further increase of these two parameters, the energy dissipation in the penetration stage becomes predominant. Finally, we developed an equation to predict the restitution coefficient of the wet normal impact with acceptable accuracy.

Keywords: Wet impact; Restitution coefficient; Stokes number; Theoretical modeling.

INTRODUCTION

It is common in real-world applications that a small amount of liquid is added into particulate processes, for example, particle synthesis and surface modification, pharmacy, and food processing. The presence of liquid makes the particles coated with liquid layers or agglomerated by liquid bridges, which results in the particulate flow behaviors greatly different from that of dry system (Seville and Clift, 1984, Mitarai and Nori, 2006; Zhu *et al.*, 2013; Zhou *et al.*, 2013; Zhou *et al.*, 2016). Particle-particle and particle-wall impacts play key roles in such flows. A detailed understanding on the individual impact with liquid is helpful to reveal the mechanisms of these flows.

Theoretical mechanisms of impacts with liquid has been an increasing interest but still in controversy, because unlike impacts between dry bodies, the introduction of viscous damping from liquid contributes to the complexity of physical description of the impact. In the literature, there are three theoretical approaches to study wet impact generally, which are (1) Direct Numerical Simulation (DNS) model of particle interface (Jain *et al.*, 2012); (2) physical modeling of different forces acting on the particle during impact (Antonyuk *et al.*, 2009), and (3) elastohydrodynamic theory or lubrication theory (Davis *et al.*, 1986).

With DNS approach, Jain *et al.* (2012) developed a combination of the Volume of Fluid (VOF) and Immersed Boundary (IB) model to simulate particle impact on thin liquid films and revealed detailed behaviors. Tobias and Jochen (2012) developed interface-resolving numerical simulations of particle-particle impacts for revealing the impact mechanisms. Since the DNS approach itself is a challenge, it is out of the scope of the present work.

By physical modeling of forces, Antonyuk *et al.* (2009) illustrated the energy balance during impact and presented a reasonable prediction of restitution coefficient. However, one weak point of their model is that it involves lots of assumption parameters, especially for the contact force model.

The elastohydrodynamic theory or lubrication theory, originally proposed by Davis and his colleagues seems an elegant method. Davis *et al.* (1986) studied theoretically a head-on impact of a sphere on a plate immersed in a viscous liquid and developed elastohydrodynamic theory to quantify rebound characteristics. According to this theory, the restitution coefficient, which is defined as the ratio of sphere velocity after impact to that before impact, can be described by Stokes number, St_d and critical Stokes number St_{dc}. St_d represents the ratio of the inertia of sphere to the viscous forces exerted by the liquid layer. St_{dc} is the critical value, below which, the kinetic energy of sphere is fully dissipated and no rebound would be observed (Barnocky and Davis, 1988).

* Corresponding author.
Tel./Fax: (+86) 25 83793453
E-mail address: dyliu@seu.edu.cn

$$St_d = \frac{mv}{6\pi\mu a^2} \tag{1}$$

$$St_{dc} = \ln(\frac{x_0}{x_1}) \tag{2}$$

$$x_1 = (4\theta\mu v a^{1.5})^{0.4} \tag{3}$$

where m is the sphere mass, v is the impact velocity, μ is the liquid viscosity, a is the sphere radius, x_0 indicates the region where the elastohydrodynamic theory is applicable. It represents the distance between sphere tip and plate surface. Basically, x_0/a should be much less than unity. x_1 is the elasticity length scale for deformation, representing the distance from the plate surface when the sphere restores enough elastic energy to rebound through deformation. $\theta = (1 - v_1^2)/\pi E_1 + (1 - v_2^2)/\pi E_2$, with E_i and v_i representing Young's modulus and Poisson's ratio for the sphere ($i = 1$) and plate ($i = 2$) respectively.

The elastohydrodynamic theory was then applied in several experiments to characterize impact processes. Joseph *et al.* (2001) performed a normal impact of a particle attached to a pendulum with a plate immersed in viscous liquid and found that no rebound is observed for $St_d < St_{dc}$. When $St_d > St_{dc}$, the restitution coefficient, e_{wet}, increases sharply before reaching a constant value. Similar experiments for immersed impact were also carried out by Gondret *et al.* (1999), Gondret *et al.* (2002) and Lundberg et al. (1992), with consistent results with the elastohydrodynamic theory.

Besides the immersed impacts, Davis *et al.* (2002) affirmed the applicability of the elastohydrodynamic theory to the impact with thin liquid layer, where the conditions are restricted to $h << a$, where h is the layer thickness. An equation was proposed to predict e_{wet} with a simple form.

$$e_{wet} = e_{dry}(1 - \frac{St_{dc}}{St_d}) \tag{4}$$

e_{dry} is the restitution coefficient for the dry impact. It is used to account for the energy dissipation in the solid.

Although the elastohydrodynamic theory has been successfully applied to various wet impacts (immersed impact and thin-layer impact), it is not appropriate for characterizing the impact between the sphere and liquid layer with considerable thickness. Briefly, the elastohydrodynamic theory neglects the effects of layer thickness in the energy dissipation, manifesting as the absence of layer thickness in the definition of St_d. However, it has been proved that the layer thickness plays an important role in the impact (Antonyuk *et al.*, 2009; Crüger *et al.*, 2015; Ma *et al.*, 2015). Therefore, in our early work (Ma *et al.*, 2013), we proposed a modified Stokes number, St_m to incorporate the effects of layer thickness:

$$St_m = \frac{mv}{\mu dh} \tag{5}$$

In the present paper, we extended elastohydrodynamic theory to thick-layer impact system by coupling the physical modeling of forces for further physical insight into the impact mechanism. The objective of the theory is two-fold: i) to predict whether the sphere would rebound after the impact; ii) to estimate the restitution coefficient. The experimental data used in the following was obtained through our previous work (Ma *et al.*, 2015).

THEORETICAL DEVELOPMENT

Critical Stokes number, St_{mc}, is usually used to predict whether the sphere would rebound subsequent to a normal impact. It is the St_m at which e just drops to zero. In order to estimate St_{mc}, we divided the whole impact process into three stages: 'penetration', 'contact' and 'rebound' as illustrated in Fig. 1. The centroid of the sphere whose tip just contacts the liquid surface is set as original point and that the downward direction is chosen as the plus direction.

The ***penetration stage*** starts from the liquid layer surface to $0.01a$ from the plate surface. The ***contact stage*** begins at $0.01a$ and ends at the elasticity length scale for deformation, x_1. Within this region, the elastohydrodynamic theory is applicable (the prime condition for the theory is $x_0 << a$. That is why we set $0.01a$ as the initial point of contact

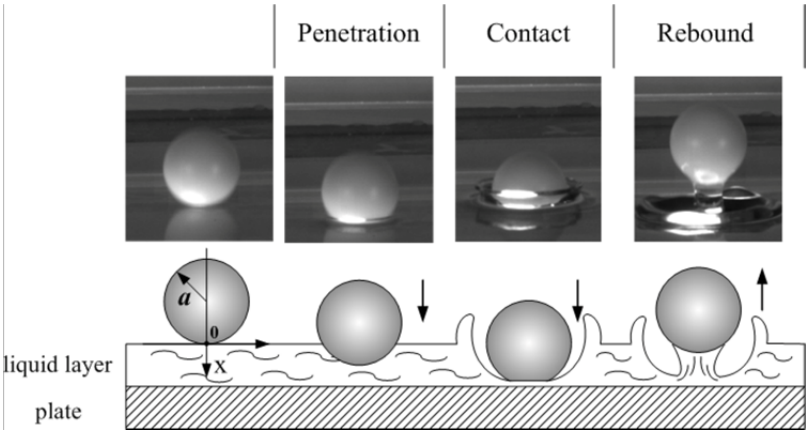

Fig. 1. Schematic representation of impact stages.

stage). The ***rebound stage*** covers the process from the formation of liquid bridge to the maximum bridge length.

In terms of impact process, the sphere velocity could drop to zero at any one of the three stages. Therefore, three critical Stokes numbers have to be developed, aiming at full absorption of kinetic energy in different stages. Previously, several assumptions have to be made as follows:

(1) The liquid layer is Newtonian fluid, namely, its rheological behavior is constant throughout the impact process.
(2) A rough calculation on the magnitude of viscous force has been made for the case that the kinetic energy of sphere is fully dissipated. It is far larger than the sphere gravity. Thus, we neglected the effects of sphere gravity in the modeling process.
(3) Surrounding air has negligible effect on the impact dynamics.

Penetration:

During the penetration stage, the kinetic equations can be approximated as:

$$\frac{dx}{dt} = v(t) \tag{6}$$

$$m\frac{dv}{dt} = F_D + F_{vis} \tag{7}$$

where m is the sphere mass, $v(t)$ is the relative velocity of the sphere toward the plate. F_D and F_{vis} are the drag force and viscous force imposed by the liquid respectively.

$$F_D(t) = \frac{1}{2}\rho_l C_D A_D v(t)^2 \tag{8}$$

Here, ρ_l is the liquid density, $A_D = \pi(2ax - x^2)$ is the characteristic area, C_D is the drag coefficient which is evaluated using the following equation:

$$C_D = \frac{24}{\mathrm{Re_p}} + \frac{4}{\sqrt{\mathrm{Re_p}}} + 0.4 \tag{9}$$

Eq. (9) is applicable for a wide range of Re_p ($0 < Re_p < (2–4) \times 10^5$) (Antonyuk *et al.*, 2009). $Re_p = d_{pe}v\rho_l/\mu$, where d_{pe} is the equivalent diameter of the immersed part of the sphere in the liquid layer. In order to simplify the modeling process, we used the length of sphere immersed in liquid, x, as the characteristic length of Reynolds number, instead of d_{pe}. Thus, the new Reynolds number is $Re_x = v\rho_l x/\mu$. Based on Re_x, a simplified form of Eq. (9) is given as follows:

$$C_D = \frac{18}{\mathrm{Re}_x} \tag{10}$$

Fig. 2 plots a comparison between the drag coefficient estimated by Eqs. (9) and (10). Within the Reynolds numbers studied, the predictions of C_D from both equations agree well. It implies that Eq. (10) could provide acceptable C_D in spite of its much more simplified form when compared with Eq. (9).

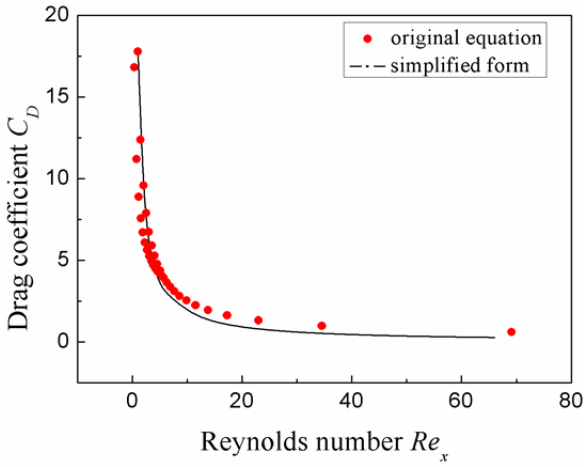

Fig. 2. Comparison between the predicted C_D from Eqs. (9) and (10).

According to Adams and Edmondson (1987), the viscous force F_{vis} can be found as:

$$F_{vis} = \frac{1.5\pi\mu a^2}{h - x}v \tag{11}$$

Therefore, dividing Eq. (7) by Eq. (6) to eliminate the time term and employing the boundary condition $v = v_0$ at $x = 0$ and $v = v_1$ at $x = h - 0.01a$ for integral, yields

$$v_1 = v_0 + \frac{1.5\pi\mu a^2 \ln\frac{x_0}{h}}{m} + \frac{4.5\mu\pi(h^2 - 4ah)}{m} \tag{12}$$

where $x_0 = 0.01a$.

Through rearranging Eq. (12), a correlation that involves St_m can be obtained as Eq. (13).

$$\begin{aligned} v_1 &= v_0[1 + \frac{\mu dh}{mv_0}\frac{1.5\pi a}{2h}\ln\frac{x_0}{h} + \frac{9\pi}{4a}(h - 4a)\frac{\mu dh}{mv_0}] \\ &= v_0\{1 + [\frac{1.5\pi a}{2h}\ln\frac{x_0}{h} + \frac{9\pi}{4a}(h - 4a)]\frac{1}{St_m}\} \end{aligned} \tag{13}$$

If the kinetic energy of the sphere is fully absorbed in this stage, $v_1 = 0$. The critical Stokes number St_{mc1} is

$$St_{mc1} = \frac{9\pi}{4a}(4a - h) - \frac{3\pi a}{4h}\ln(\frac{x_0}{h}) \tag{14}$$

Contact:

According to the elastohydrodynamic theory (Davis *et al.*, 2002), the reduction of sphere velocity in the contact stage is given:

$$\frac{v_2}{v_1} = e_{dry}(1-\frac{St_{dc}}{St_d}) \quad (15)$$

v_2 is the sphere velocity at the beginning of the rebound. It can be calculated by combining Eqs. (13) and (15) as:

$$v_2 = [v_0 + \frac{1.5\pi\mu a^2 \ln\frac{x_0}{h}}{m} + \frac{4.5\mu\pi(h^2-4ah)}{m}]e_{dry}(1-\frac{St_{dc}}{St_d}) \quad (16)$$

If $v_2 = 0$ but $v_1 \neq 0$, the kinetic energy of sphere is dissipated in the contact stage, where $St_d < St_{dc}$ (Barnocky and Davis, 1988) is met.

Rebound:

As can be seen from Fig. 1, due to the effect of liquid inertia, the liquid would propagate away with higher amplitude than layer thickness during the penetration and contact stages. It results in that the amount of liquid acting on the sphere in the rebound process is much smaller. In this regard, the main resistance acting on the sphere could only be liquid bridge force instead of drag force and viscous force.

The liquid bridge force could be divided into dynamic force and static force. For a dynamic bridge, the former is much larger than the latter (Ennis *et al.*, 1990; Pitois *et al.*, 2000). Therefore, in the present paper, we incorporated the dynamic liquid bridge force into the model.

According to Matthewson (1988), for a thin-layer impact, the dynamic liquid bridge force can be approximated as:

$$F_L = 6\pi\mu v a^2(1-\frac{D}{H})^2\frac{1}{D} \quad (17)$$

H is the distance from the plate surface at wetted radius r, D is the distance between the sphere tip and plate surface (Fig. 3).

We estimated H-D as layer thickness h. The length that liquid bridge force imposes over is L_{max} which is the maximum length of the liquid bridge throughout the impact. Based on the previous experimental work, we plotted L_{max} as a function of St_m in Fig. 4. St_m is plotted in a logarithmic way to cover a wide range of values where the liquid viscosity ranges from 7 mPa.s to 2040 mPa.s and layer thickness in the range of 0.5 mm to 3 mm. As can be seen, taking St_m = 210 as the cut-off point, L_{max} increases first then falls algebraically with St_m. The non-linear variation of L_{max} corresponds to two bridge status: rupture and non-rupture. When St_m < 210, the liquid bridge force is large enough to dissipate all the kinetic energy of sphere, thus no ruptures were observed. The decline of resistance associating with the increasing of St_m lowers the decay rate of kinetic energy, therefore causing an increase of L_{max}. With further increase of St_m beyond 210, the liquid bridge would rupture before the sphere is brought to rest, when the kinetic energy of sphere E_r exceeds the rupture energy of bridge E_{rup}. The increasing of St_m reduces E_{rup}, causing the point where $E_r > E_{rup}$ occur in advance, which results in a decline of L_{max}. It is consistent with the demonstrations of Pitois *et al.* (2001) and Lian *et al.* (1993). Based on the experimental data, two equations are fitted for both cases respectively:

$$L_{\max} = 0.0146\ln(St_m) - 0.046 \quad St_m < 210 \quad (18)$$

$$L_{\max} = -0.0073\ln(St_m) + 0.0857 \quad St_m \geq 210 \quad (19)$$

On the basis of kinetic equations, Eqs. (20) and (21) are obtained for the rebound stage:

$$\int_{v2}^{v3} dv = \frac{6\pi\mu a^2}{m}\int_h^{L_{\max}+h}(1-\frac{D}{D+h})^2\frac{1}{D}dD \quad (20)$$

$$v_3 = v_2 - \frac{6\pi\mu a^2}{m}[\ln(\frac{L_{\max}+h}{L_{\max}+2h}) + \frac{h}{L+2h} + \ln 2 - \frac{1}{2}] \quad (21)$$

If the sphere velocity is brought to 0 in the rebound stage, v_3 = 0. Thus, the critical Stokes number in this stage, St_{mc2} can be achieved by combining Eqs. (13), (15) and (21):

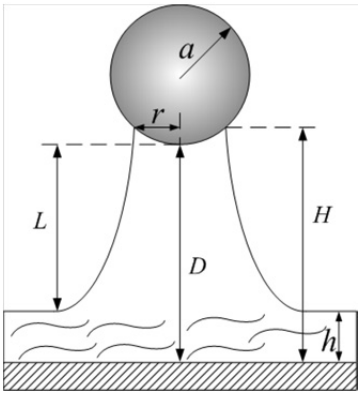

Fig. 3. Geometry of liquid bridge.

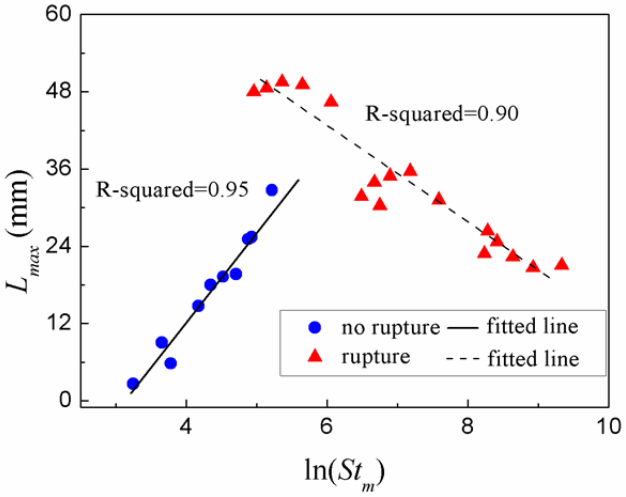

Fig. 4. Maximum length of liquid bridge, L_{max} versus St_m for normal impact with an impact velocity of 2.28 m s^{-1}.

$$St_{mc2} = \frac{\frac{3\pi a \ln\frac{x_0}{h}}{4h} + \frac{9\pi}{4a}(h-4a)}{\frac{\ln(\frac{L_{\max}+h}{L_{\max}+2h}) + \frac{h}{L+2h} + \ln 2 - \frac{1}{2}}{e_{dry}(St_d - St_{dc})} - 1} \quad (22)$$

Basically, whether the sphere would rebound subsequent to a normal impact mainly depends on the comparisons of St_m with three critical Stokes numbers. If $St_m > St_{mc1}$, the sphere would pass the first stage with certain velocity. Then calculate the sphere velocity after penetration stage, v_1 using Eq. (12) and compare St_d with St_{dc} based on v_1. If $St_d > St_{dc}$, the sphere could depart from the plate after contact stage. Finally, compare St_m with St_{mc2} that is calculated with v_2 from Eq. (16). If $St_m > St_{mc2}$, rebound occurs. Generally, the expectation that the sphere rebounds out of liquid layer must full fill the fact that the Stokes numbers are larger than the critical values for all the three stages. If not, the sphere velocity would be brought to zero in the corresponding stage.

DISCUSSION

Critical Stokes Number

Fig. 5 plots a comparison between experimental and theoretical St_{mc}. As can be seen, the experimental data, in spite of their scatter, shows reasonable agreement with the theoretical predictions. The scatter may be attributable to the negligence of liquid inertia in the modeling process. In the present work, the effect of liquid inertia is only used to determine the resistance involved in the rebound stage. However, from rough observation, it can be confirmed that the liquid inertia also influences the penetration stage. Therefore, improving the physical models by incorporating the liquid inertia could enhance the predictability of the overall models.

Of significant practical interest is realizing the effects of various impact parameters on St_{mc} which concerns whether a sphere would stick to the plate after impact. We used Eqs. (14) and (22) to calculate St_{mc1} and St_{mc2} and study how they change with physical parameters.

Fig. 6 shows the critical Stokes number for the penetration stage, St_{mc1}, as a function of layer thickness, h and sphere radius, a. The variation of St_m is also plotted in Fig. 6 for comparison. As can be seen, St_{mc1} decreases with the layer thickness while increases with the sphere radius. As h increases within a low level, St_m is larger than St_{mc1}, implying that the sphere would go through the penetration stage with certain kinetic energy (Fig. 6(a)). With further growth of h, St_m decreases more sharply than St_{mc1}. When h increases beyond a critical point, St_m is smaller than St_{mc1}. The sphere velocity would be brought to zero in this stage and no rebound can be observed. The critical point inversely depends on the liquid viscosity. Opposite trend is found regarding the effects of sphere radius (Fig. 6(b)). The sphere inertia decreases with a, leading to a smaller St_m as compared with St_{mc1} and full dissipation of kinetic energy in this stage. Until the radius increases beyond a critical point, St_m exceeds

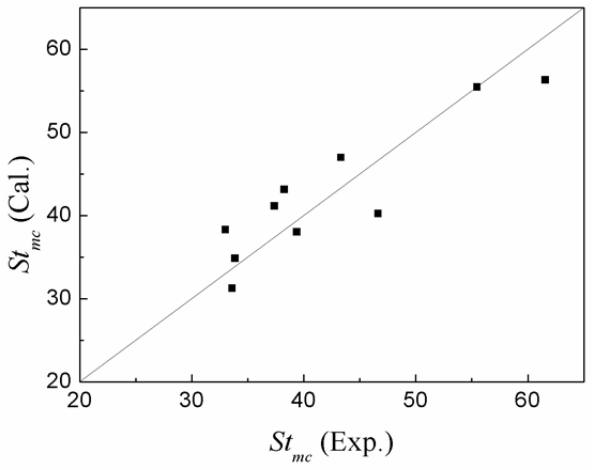

Fig. 5. Critical Stokes numbers, St_{mc}, decided by experiment versus theoretical predictions given by Eqs. (14) and (22).

St_{mc1}, making rebound possible. Different from Fig. 6(a), the critical sphere radius increases with the liquid viscosity.

Fig. 7 shows the critical Stokes number for the rebound stage, St_{mc2}, as a function of layer thickness and sphere radius. Non-linear variation of St_{mc2} is observed. It is mainly caused by different sensitivities to the impact parameters between penetration and rebound stages. Different from St_{mc1}, St_{mc2} increases with liquid viscosity. The cross point between St_m and St_{mc2} moves toward smaller thickness as the liquid viscosity increases, indicating an increasing trend for the full dissipation of kinetic energy

Fig. 8 provides a comparison of the percentages of initial impact energy that are dissipated in the penetration, contact and rebound stages as a function of layer thickness and liquid viscosity. When the layer thickness ranges below 0.3 mm, the energy dissipated in the contact stage is the largest, indicating a predominant role of lubrication force (Davis *et al.*, 1986). The percentage for the rebound stage is the smallest throughout. It implies that liquid bridge force makes less contribution to the energy dissipation as compared with drag force, viscous force and lubrication force. As the thickness further increases, the dissipative percentage in the penetration stage sharply increases, whereas the percentages of contact stage and rebound stage decrease monotonically. When the layer thickness exceeds 1.6 mm, the percentage of dissipative energy in the rebound stage becomes zero, implying that the sphere velocity is reduced to zero in the contact stage. At this point, most of kinetic energy is dissipated in the penetration stage. Similar trends can be observed considering the effects of liquid viscosity (Fig. 8(b)). Note that, the contribution of rebound stage and contact stage to the energy dissipation increases first with the liquid viscosity then decreases. Taking the contact stage as an example, the percentage of energy loss in this stage is defined as: $R = (v_1^2 - v_2^2)/v_0^2$ where v_0, v_1 and v_2 are the sphere velocity at the layer surface, at the beginning and the end of the contact stage respectively. With the increasing of liquid viscosity, the energy loss in the penetration stage increases and thus the sphere velocity at the end of this stage, viz. at the beginning of the contact stage decreases. Even so, the

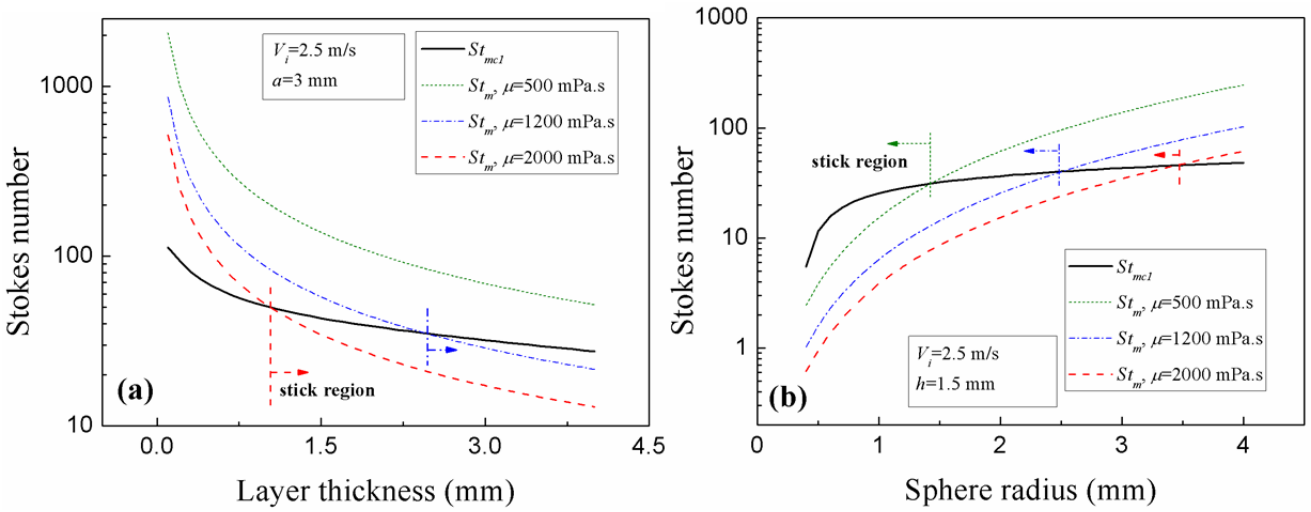

Fig. 6. Critical Stokes number for the penetration stage as a function of impact parameters. (a) liquid layer thickness; (b) sphere radius.

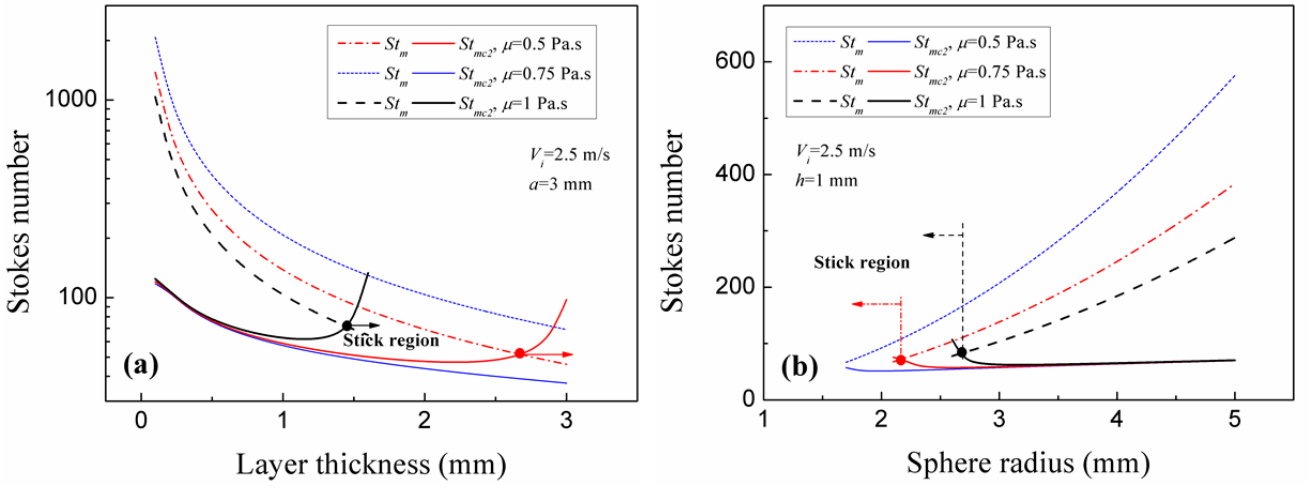

Fig. 7. Critical Stokes number for rebound stage as a function of impact parameters. (a) liquid layer thickness; (b) sphere radius.

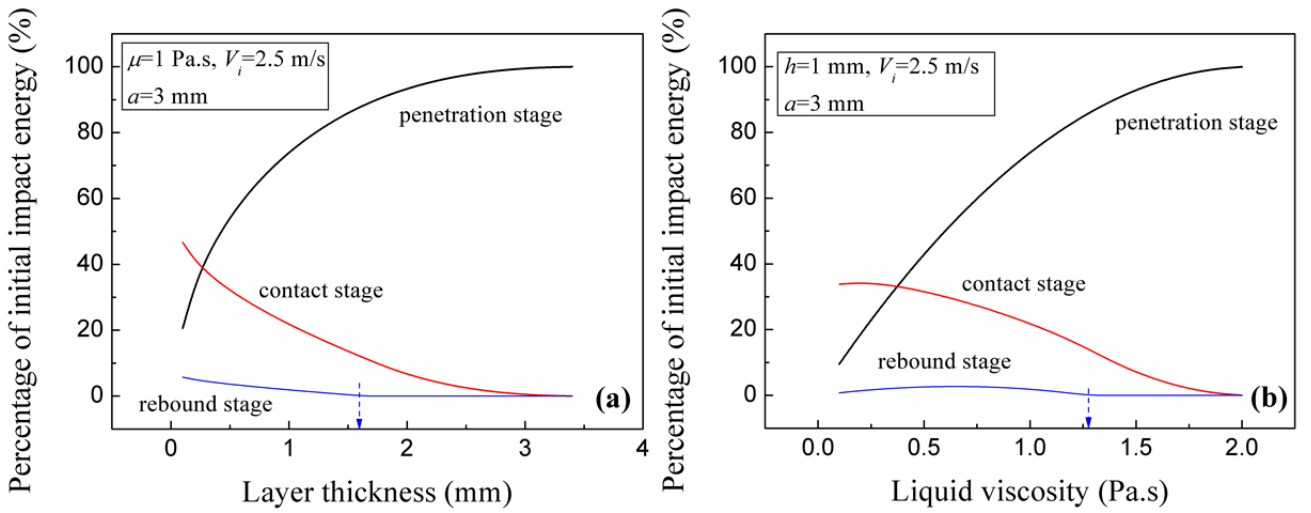

Fig. 8. Percentage of initial impact energy that is dissipated in each stage as a function of liquid properties. (a) layer thickness; (b) liquid viscosity.

energy loss in the contact stage still increases with liquid viscosity. This indicates that although v_1 decreases with increasing liquid viscosity, v_2 decreases more. Therefore, it can be concluded that the energy dissipation caused by the lubrication force (contact stage) is more sensitive to the liquid viscosity as compared with the penetration stage. Based on the same reason, similar conclusion may be drawn regarding the rebound stage.

Restitution Coefficient

Regarding the impact on a liquid layer with large thickness, the effect of liquid bridge has to be considered since it also makes contribution to the energy dissipation. Therefore, the restitution coefficient in the present paper is defined as the ratio of the sphere velocity at the bridge rupture, V_r, to the impact velocity, V_i.

$$e = \frac{V_r}{V_i} \tag{23}$$

Due to the inapplicability of existing models in characterizing the "thick-layer impact" (Ma *et al.*, 2015), we tried to derive a new equation to predict restitution coefficient based on St_m. Fig. 9 plots the dependence of restitution coefficient, e on St_m for normal impact with different velocities. As can be seen, the data shows less scatter when compared to that scaling with St_d (Ma *et al.*, 2015), implying a good applicability of St_m in describing the "thick-layer impact". Moreover, from a qualitative perspective, Fig. 9 shares some similarities with those obtained previously for thin-layer impact (Davis *et al.*, 2002; Kantak and Davis, 2004; Gollwitzer *et al.*, 2012). Thus, the equation for "thick-layer impact" can be given in analogy with Eq. (4) by incorporating the modified Stokes number St_m and St_{mc}. It is worth pointing out that e_{dry} in Eq. (4) serves as a reduction factor to characterize the energy dissipation in the solid. Basically, this factor should

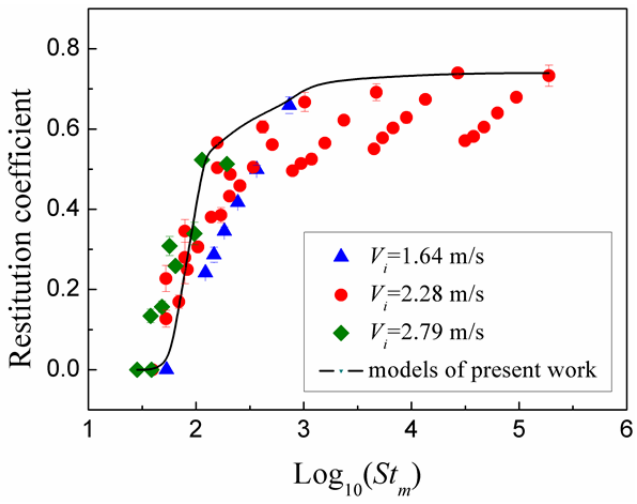

Fig. 9. Comparison between experimental and theoretical restitution coefficients of normal impact as a function of St_m.

involve all the other factors that cause energy dissipation except viscous damping from liquid. For the impact with liquid, using e_{dry} as the reduction factor is not appropriate, because the presence of liquid can not only cause energy loss through viscous force, but also affect the pressure profile over the sphere surface, thereby changing the deformation and rebound velocity of the sphere. In this regard, e_{dry} has to be replaced by a new value to involve the effects of liquid on the energy dissipation in the solid. In the present work, we used the restitution coefficient of the impact on a 0.5 mm of water layer ($e_w \approx 0.74$) as the new reduction factor, because e_w almost excludes the effect of liquid viscous force due to the small layer thickness and viscosity, and only represents the energy dissipation in the solid.

$$e_{wet} = e_w\left(1 - \frac{St_{mc}}{St_m}\right) \tag{24}$$

where St_{mc} is the critical Stokes number calculated using Eq. (22). The predicted restitution coefficients are also plotted in Fig. 9. Apparently, it agrees much better with the experimental values than any other models. Only a bit of overestimations are observed at large St_m. It should be closely related to the negligence of liquid inertia under high St_m especially for the cases with large layer thicknesses. That is also one cause for the scatter of data in Fig. 9. Therefore, further work will aim at improving Eq. (24) to reduce the data scatter and enhance its predictability.

CONCLUSION

Aiming at normal impact between dry sphere and liquid layer with considerable thickness, the present paper extended elastohydrodynamic theory by coupling the physical force models to reveal the detailed impact mechanism. Based on the theoretical work, the following conclusions are drawn:

(1) Three critical Stokes numbers, St_{mc1}, St_{dc} and St_{mc2} are developed corresponding to the penetration, contact and rebound stages respectively. The Stokes numbers and critical values are compared to determine whether the sphere would rebound after the impact.

(2) St_{mc1} decreases with increasing layer thickness while increases with sphere radius. Non-linear dependence of St_{mc2} on the layer thickness and sphere radius are observed. Increasing layer thickness would facilitate the sticking of sphere on the liquid layer. Moreover, the effects are enhanced by increasing the liquid viscosity. Opposite trends are observed regarding the effect of sphere radius.

(3) When the layer thickness and liquid viscosity are changed within a low level, most of the kinetic energy is dissipated in the contact stage. However, with further increase of these two parameters, the energy dissipation in the penetration stage becomes predominant while the dissipation in the contact and rebound stage keeps decreasing till to zero.

(4) An equation is proposed to estimate the restitution coefficient of the wet normal impact with considerable

liquid layer thickness. It provides more accurate predictions than the existing models which are applicable for "thin-layer impact".

ACKNOWLEDGEMENT

This work was financially supported by the National Natural Science Foundation of China (No. 51306035) and Scientific Research Foundation of Graduate School of Southeast University.

REFERENCE

Adams, M.J. and Edmondson, B. (1987). In *Tribology in particulate technology*, Briscoe, B.J. and Adams, M.J. (Eds.), Adam Hilger, Bristol and Philadelphia, p.154.

Antonyuk, S., Heinrich, S., Deen, N. and Kuipers, H. (2009). Influence of liquid layers on energy absorption during particle impact. *Particuology* 7: 245–259.

Barnocky, G. and Davis, R.H. (1988). Elastohydrodynamic collision and rebound of spheres: Experimental verification. *Phys. Fluids* 31: 1324–1329.

Crüger, B., Salikov, V., Heinrich, S., Antonyuk, S., Sutkar, V.S., Deen, N.G. and Kuipers, J.A.M. (2015). Coefficient of restitution for particles impacting on wet surfaces: An improved experimental approach. *Particuology* 25: 1–9, doi: 10.1016/j.partic.2015.04.002.

Davis R.H., Serayssol, J.M. and Hinch, E.J. (1986). Elastohydrodynamic collision of two spheres. *J. Fluid Mech.* 163: 479–497.

Davis R.H., Rager D.A. and Good B.T. (2002). Elastohydrodynamic rebound of spheres from coated surfaces. *J. Fluid Mech.* 468:107–119.

Ennis, B.J., Li, J., Gabriel, I.T. and Robert, P. (1990). The influence of viscosity on the strength of an axially strained pendular liquid bridge. *Chem. Eng. Sci.* 45: 3071–3088.

Gollwitzer, F., Rehberg, I., Kruelle, C.A. and Huang, K. (2012). Coefficient of restitution for wet particles. *Phys. Rev. E* 86: 011303.

Gondret, P., Hallouin, E., Lance, M. and Petit, L. (1999). Experiments on the motion of a solid sphere toward a wall: From viscous dissipation to elastohydrodynamic bouncing. *Phys. Fluids* 11: 2803–2805.

Gondret, P., Lance, M. and Petit, L. (2002). Bouncing motion of spherical particles in fluids. *Phys. Fluids* 14: 643–652.

Jain, D., Deen, N.G., Kuipers, J.A.M., Antonyuk, S. and Heinrich, S. (2012). Direct numerical simulation of particle impact on thin liquid films using a combined volume of fluid and immersed boundary method. *Chem. Eng. Sci.* 69: 530–540.

Joseph, G.G., Zenit, R., Hunt, M.L. and Rosenwinkel, A.M. (2001). Particle-wall collisions in a viscous fluid. *J. Fluid Mech.* 433: 329–346.

Joseph, G.G. and Hunt, M.L. (2004). Oblique particle-wall collisions in a liquid. *J. Fluid Mech.* 510: 71–93.

Kantak, A.A. and Davis, R.H. (2004). Oblique collisions and rebound of spheres from a wetted surface. *J. Fluid Mech.* 509: 63–81.

Lian, G., Thornton, C. and Adams, M.J. (1993). A theoretical study of the liquid bridge forces between two rigid spherical bodies. *J. Colloid Interface Sci.* 161: 138–147.

Lundberg, J. and Shen, H. (1992). Collisional restitution dependence on viscosity. *J. Eng. Mech.* 118: 979–989.

Ma, J., Liu, D. and Chen, X. (2015). Normal and oblique impacts between smooth spheres and liquid layers: Liquid bridge and restitution coefficient. *Powder Technol.*, *in submission.*

Matthewson, M.J. (1988). Adhesion of spheres by thin liquid films. *Philos. Mag. A.* 57: 207–216.

Mitarai, N. and Nori, F. (2006). Wet granular materials. *Adv. Phys.* 55: 1–45.

Pitois, O., Moucheront, P. and Chateau, X. (2000). Liquid Bridge between two moving spheres: An Experimental study of viscosity effects. *J. Colloid Interface Sci.* 231: 26–31.

Pitois, O., Moucheront, P. and Chateau, X. (2001). Rupture energy of a pendular liquid bridge. *Eur. Phys. J. B* 23: 79–86.

Seville, J.P.K. and Clift, R. (1984). The effect of thin liquid layers on fluidisation characteristics. *Powder Technol.* 37: 117–129.

Tobias, K. and Jochen, F. (2012). Collision modelling for the interface-resolved simulation of spherical particles in viscous fluids. *J. Fluid Mech.* 709: 445–489.

Zhou, Y., Ren, C., Wang, J. and Yang, Y. (2013). Characterization on hydrodynamic behavior in liquid-containing gas-solid fluidized bed reactor. *AIChE J.* 59: 1056–1065.

Zhou, Y., Shi, Q., Huang, Z., Wang, J. and Yang, Y. (2016). Effects of liquid action mechanisms on hydrodynamics in liquid-containing gas–solid fluidized bed reactor. *Chem. Eng. J.* 285: 121–127.

Zhu, R., Li, S and Yao, Q. (2013). Effects of cohesion on the flow patterns of granular materials in spouted beds. *Phys. Rev. E* 87: 022206.

Received for review, August 29, 2015
Revised, December 4, 2015
Accepted, December 4, 2015